Carcinogenesis vol.29 no.5 pp.1077–1082, 2008
doi:10.1093/carcin/bgn069
Advance Access publication March 20, 2008

The aryl hydrocarbon receptor (AhR) inhibits vanadate-induced vascular endothelial growth factor (VEGF) production in TRAMP prostates

Wayne A.Fritz[1], Tien-Min Lin[1] and Richard E.Peterson[1,2,*]

[1]School of Pharmacy and [2]Molecular and Environmental Toxicology Center, University of Wisconsin, 777 Highland Avenue, Madison, WI 53705, USA

*To whom correspondence should be addressed. Tel: +1 608 263 5453; Fax: +1 608 265 3316;
Email: repeterson@pharmacy.wisc.edu

Hypoxia-inducible factor-1 alpha (HIF-1α) and aryl hydrocarbon receptor nuclear translocator (ARNT) are basic helix-loop-helix/per-arnt-sim (PAS) family transcription factors. During angiogenesis and tumor growth, HIF-1α dimerizes with ARNT, inducing expression of many genes, including vascular endothelial growth factor (VEGF). ARNT also dimerizes with the aryl hydrocarbon receptor (AhR). AhR-null (*Ahr*$^{-/-}$) transgenic adenocarcinoma of the mouse prostate (TRAMP) mice develop prostate tumors with greater frequency than AhR wild-type (*Ahr*$^{+/+}$) TRAMP mice, even though prevalence of prostate epithelial hyperplasia is not inhibited. This suggests that *Ahr* inhibits prostate carcinogenesis. In TRAMP mice, prostatic epithelial hyperplasia results in stabilized HIF-1α, inducing expression of VEGF, a prerequisite for tumor growth and angiogenesis. Since ARNT is a common dimerization partner of AhR and HIF-1α, we hypothesized that the AhR inhibits prostate tumor formation by competing with HIF-1α for ARNT, thereby limiting VEGF production. Prostates from *Ahr*$^{+/+}$, *Ahr*$^{+/-}$ and *Ahr*$^{-/-}$ C57BL/6J TRAMP mice were cultured in the presence of graded concentrations of vanadate, an inducer of VEGF through the HIF-1α–ARNT pathway. Vanadate induced VEGF protein in a dose-dependent fashion in *Ahr*$^{+/-}$ and *Ahr*$^{-/-}$ TRAMP cultures, but not in *Ahr*$^{+/+}$ cultures. However, vanadate induced upstream proteins in the phosphatidylinositol 3-kinase-signaling cascade to a similar extent in TRAMPs of each *Ahr* genotype, evidenced by v-akt murine thymoma viral oncogene homolog (Akt) phosphorylation. These findings suggest that AhR sequesters ARNT, decreasing interaction with HIF-1α reducing VEGF production. Since VEGF is required for tumor vascularization and growth, these studies further suggest that reduction in VEGF correlates with inhibited prostate carcinogenesis in *Ahr*$^{+/+}$ TRAMP mice.

Introduction

Recent estimates indicate that prostate cancer is the most common non-cutaneous cancer diagnosed annually and is the second leading cause of cancer death in American men (1). It is believed that human prostate cancer originates from high-grade prostatic intraepithelial neoplasia lesions (2,3) that progress through distinct morphological stages to clinical disease. A shift toward androgen-independence occurs in the progression of these microscopic lesions to advanced prostate cancer, correlating with greater metastatic potential (4,5).

Angiogenesis plays an integral role in tumor growth and progression (6,7). Vascular endothelial growth factor (VEGF) is the major growth factor that regulates angiogenesis and tumor growth (8). VEGF expression correlates with greater microvessel density and an unfavorable prognosis in patients with prostate cancer (9–12). VEGF is transcriptionally regulated by hypoxia-inducible factor-1 alpha (HIF-1α) in response to tissue hypoxia (13,14) and through activation of the phosphatidylinositol 3-kinase (PI3K)/v-akt murine thymoma viral oncogene homolog (Akt) survival signaling pathways (15,16). HIF-1α activation (17) and PI3K signaling (18) have been implicated in several human cancers, including those of the prostate.

Tissue hypoxia stabilizes HIF-1α, which forms heterodimers with HIF-1β, also known as the aryl hydrocarbon receptor nuclear translocator (ARNT). Activation of this pathway induces VEGF production. ARNT also heterodimerizes with the aryl hydrocarbon receptor (AhR) (19), a basic helix-loop-helix ligand-activated transcription factor. Although the most well-defined role of the AhR is binding to several environmental toxins including polychlorinated dibenzo-*p*-dioxins and dibenzofurans, an endogenous ligand for the AhR has recently been identified (20,21). Both the AhR and ARNT are expressed in benign prostatic hyperplasia and in prostate cancer in humans (22), suggesting that the AhR may be implicated in prostate carcinogenesis.

Identification of the role of the AhR in normal developmental processes has been facilitated by the availability of mice lacking the AhR (*Ahr*$^{-/-}$) (23–25). In a recent study using a genetic cross between AhR-null mice and the transgenic adenocarcinoma of the mouse prostate (TRAMP) model of prostate cancer (26–29), we showed that the presence of the *Ahr* inhibited the formation of prostate tumors possessing a neuroendocrine phenotype (30). Although all mice had diffuse epithelial hyperplasia in the dorsolateral prostate characteristic of the TRAMP model by 105 days, *Ahr*$^{+/+}$ TRAMP mice had reduced tumor incidence by 140 days of age. Immunohistochemical studies have shown that neuroendocrine cells are androgen receptor negative and colocalize with VEGF (9,10,31). This suggests that the AhR could inhibit prostate tumor growth in TRAMP mice by regulating VEGF production.

Because HIF-1α and the AhR share a common dimerization partner, it is possible that interaction between the AhR and ARNT in *Ahr*$^{+/+}$ TRAMPs renders them less susceptible to increasing HIF-1α activity during carcinogenic progression in the TRAMP model (32) than *Ahr*$^{-/-}$ TRAMPs. Thus, AhR–ARNT interaction could inhibit VEGF production, similar to the effect reported previously in the heart (33), resulting in the prevention of tumor growth beyond microscopic lesions. Inhibition of VEGF production by the AhR has been associated with cardiac hypertrophy that develops in AhR-null mice (33). When the AhR is absent, cardiac hypertrophy is accompanied by greater HIF-1α levels and a subsequent increase in VEGF messenger RNA abundance. Because *Ahr*$^{-/-}$ TRAMPs could be more susceptible to increasing HIF-1α activity than *Ahr*$^{+/+}$ TRAMPs, we developed a culture method to investigate this proposed mechanism. Based on a previous observation that sodium orthovanadate stimulated the PI3K pathway and HIF-1α-induced VEGF secretion (34), we have applied this system to the cultured TRAMPs to quantitatively investigate regulation of the HIF-1α pathway by the AhR.

Using this model, we demonstrate that *Ahr*$^{+/+}$ TRAMPs are less sensitive to vanadate-induced VEGF production than *Ahr*$^{+/-}$ and *Ahr*$^{-/-}$ TRAMPs. Furthermore, we demonstrate that ARNT and HIF-1α levels are the same in *Ahr*$^{+/+}$, *Ahr*$^{+/-}$ and *Ahr*$^{-/-}$ TRAMPs and that vanadate stimulated upstream signaling in the PI3K pathway to a similar extent in TRAMPs of each *Ahr* genotype. These findings suggest that inhibition of prostate carcinogenesis in *Ahr*$^{+/+}$ TRAMP mice may result from increased AhR–ARNT interaction, reducing the amount of ARNT available to interact with HIF-1α, in turn reducing VEGF production and subsequent tumor growth.

Abbreviations: AhR, aryl hydrocarbon receptor; ARNT, aryl hydrocarbon receptor nuclear translocator; Akt, v-akt murine thymoma viral oncogene homolog; HIF-1α, hypoxia-inducible factor-1 alpha; PI3K, phosphatidylinositol 3-kinase; TBST, tris-buffered saline tween-20; TRAMP, transgenic adenocarcinoma of the mouse prostate; VEGF, vascular endothelial growth factor.

Materials and methods

Transgenic mice

Animal care and use procedures were in accordance with the University of Wisconsin-Madison Research Animal Care and Use Committee guidelines and the National Institutes of Health Guide for the Care and Use of Laboratory

Animals. Mice were housed in clear plastic cages with heat-treated chipped aspen bedding in rooms maintained at 24 ± 1°C with a 12 h light–dark cycle (lighted from 6 a.m. to 6 p.m.). Feed (5015 Mouse Diet, PMI Nutrition International, Brentwood, MO) and tap water were available *ad libitum*. C57BL/6-Tg(TRAMP)8247Ng/J mice backcrossed to a C57BL/6J background for at least 20 generations (stock number 003135, Jackson Laboratories, Bar Harbor, ME) were obtained from Dr George Wilding (School of Medicine and Public Health, University of Wisconsin, Madison, WI). AhR-null mice ($Ahr^{-/-}$) backcrossed to a C57BL/6J background for at least 15 generations were obtained from Dr Christopher Bradfield (Department of Oncology, University of Wisconsin). *Ahr* genotype was determined by polymerase chain reaction analysis of DNA from an ear punch taken at 10–16 days of age (35). TRAMP transgene DNA was measured by quantitative real-time LightCycler polymerase chain reaction using primers described by Greenberg *et al.* (26) and cytokeratin 8 primers as the loading control (36).

Female TRAMP mice heterozygous for the probasin-driven SV40 T antigen were bred with C57BL/6J $Ahr^{-/-}$ males to generate $Ahr^{+/-}$ $TRAMP^{+/-}$ offspring. Mice were weaned at 21 days of age and a maximum of four males were housed in one microisolation cage until used. At sexual maturity, these mice were crossed to obtain $Ahr^{+/-}$ $TRAMP^{+/+}$ male mice, which were bred with $Ahr^{+/-}$ $TRAMP^{-/-}$ female mice to obtain experimental males that were $TRAMP^{+/-}$ and $Ahr^{+/+}$, $Ahr^{+/-}$ or $Ahr^{-/-}$.

Characterization of the effects of vanadate on VEGF secretion from $Ahr^{+/+}$ and $Ahr^{+/-}$ and $Ahr^{-/-}$ TRAMP organ cultures

At 140 days of age, dorsolateral prostates were dissected from $Ahr^{+/+}$, $Ahr^{+/-}$ and $Ahr^{-/-}$ TRAMP mice without palpable prostate tumors, placed in ice-cold Hanks' balanced salt solution containing antibiotics/antimycotics (Gibco Invitrogen Corporation, Grand Island, NY) and minced into small (~2 to 4 mg) pieces. From a previous experiment (30), it was determined that 140 days of age was the earliest day that significant differences in prostate tumor incidence occurred in $Ahr^{+/+}$, $Ahr^{+/-}$ and $Ahr^{-/-}$ TRAMP mice. Two pieces from the dorsolateral lobe of each prostate were transferred to a 24-well culture plate with 1 ml Dulbecco's modified Eagle's medium: F12 (with L-glutamine, Mediatech, Herndon, VA) culture media (1:1, vol:vol) containing 10% charcoal–dextran-stripped fetal bovine serum (Fisher Scientific, Pittsburgh, PA), antibiotics/antimycotics, insulin/transferrin/selenium (Gibco Invitrogen Corporation), 10^{-8} M 5α-dihydrotestosterone (Sigma-Aldrich Co., St. Louis, MO) and 0, 25, 50 or 100 μM vanadate (Sigma-Aldrich Co.). For inhibition of vanadate activity, pieces of minced prostate from the same dorsolateral prostate were also incubated with 100 μM vanadate plus 10, 50, 100 or 200 μM wortmannin (Sigma-Aldrich Co.). Because each dorsolateral prostate contributed duplicate pieces for each of the treatment groups, comparisons of the effects of vanadate and wortmannin on VEGF production could be made with the same prostate exposed to vehicle alone, allowing each prostate to serve as its own control. Dorsolateral prostate pieces were maintained in organ culture for 3 days, with media changed every 24 h. The media from the last 24 h incubation was used for VEGF analysis. After 3 days in culture, prostate pieces were weighed so that VEGF concentrations could be normalized to individual sample weight, and then flash frozen in liquid nitrogen for subsequent analysis.

Sample preparation

Frozen 105- and 140-day $Ahr^{+/+}$, $Ahr^{+/-}$ and $Ahr^{-/-}$ TRAMP dorsolateral prostates or 140-day dorsolateral prostate cultures were homogenized in lysis buffer containing 0.1% Triton X-100 and protease inhibitors using a Tissumizer homogenizer (Tekmar, Cincinnati, OH). Cellular debris was removed by 10 min centrifugation at 12 000 r.p.m. on a tabletop centrifuge. Tissue homogenate protein concentrations were determined using the Pierce BCA kit (South San Francisco, CA). For enzyme-linked immunosorbent assay analyses, tissue homogenates were diluted in the appropriate buffer according to the manufacturer's protocol. For western blot analysis, homogenates were boiled in sample buffer (containing 10% β-mercaptoethanol and 10% sodium dodecyl sulfate) and frozen at −20°C.

Enzyme-linked immunosorbent assay

VEGF and total HIF-1α concentrations were measured using ELISA kits (R&D Systems, Minneapolis, MN) according to the manufacturer's instructions. Whole-prostate tissue homogenates containing 40 μg of total protein (10 μg total protein for cultured prostates) were increased to a final volume of 16 μl by adding lysis buffer, eliminating potential alterations to binding efficiency caused by adding differing volumes of lysis buffer. Absorbance was measured at 450 nm with correction wavelength set at 540 nm. Sample concentrations were calculated from values obtained from the standard curve.

Western blot analysis

For each sample, 10 μg total protein was separated by sodium dodecyl sulfate–polyacrylamide gel electrophoresis and transferred to a hybond membrane (Amersham Biosciences, Piscataway, NJ) on a semidry blotting unit (Fisher Scientific). Non-specific antibody binding was blocked by 5% non-fat dry milk in tris-buffered saline tween-20 (TBST). Primary antibodies for ARNT (Santa Cruz Biotechnology, Santa Cruz, CA, diluted 1:1000), Akt and phosphorylated Akt (Cell Signaling Technology, Beverly, MA, diluted 1:200) and β-actin (Cell Signaling Technology, diluted 1:1000) in TBST containing 3% non-fat dry milk were incubated overnight at 4°C. Membranes were washed with TBST prior to incubation with the appropriate horseradish peroxidase-conjugated secondary antibody (Zymed, San Francisco, CA, diluted 1:2000) in blocking buffer. Membranes were washed again with TBST, and bands were detected using hyperfilm exposed to chemiluminescent substrate (Pierce). Band intensity was determined using ImageQuant TL software (Amersham Biosciences) and expressed relative to β-actin protein levels for each sample.

Statistical analysis

Data were analyzed for statistical significance using SigmaStat software (Jandel Scientific, San Rafael, CA). Analysis of variance was conducted on parametric data that passed Levene's test for homogeneity of variance and were normally distributed. If a significant effect was found, the least significant difference test was used to determine which groups differed from the appropriate control group. Kruskal–Wallis one-way analysis of variance on ranks was utilized for comparisons without normal distribution. Significance was set at $P < 0.05$ for all tests.

Results

VEGF concentrations in $Ahr^{+/+}$, $Ahr^{+/-}$ and $Ahr^{-/-}$ TRAMP dorsolateral prostates at 105 and 140 days of age

Prostatic VEGF concentrations in $Ahr^{+/+}$, $Ahr^{+/-}$ and $Ahr^{-/-}$ TRAMP mice at 105 and 140 days of age are shown in Figure 1. VEGF concentrations are elevated in $Ahr^{+/+}$, $Ahr^{+/-}$ and $Ahr^{-/-}$ TRAMP mouse dorsolateral prostates between 140 and 105 days of age. However, VEGF concentrations did not significantly differ between *Ahr* genotype at either 105 or 140 days of age.

Vanadate-induced VEGF production in an $Ahr^{+/-}$ TRAMP mouse dorsolateral prostate over time

Although VEGF production increases with age in prostates of all TRAMP mice prior to prostate tumor formation, it is difficult to definitively explain how mice of each *Ahr* genotype respond to activation of the angiogenesis signaling cascade. To identify how the presence of the *Ahr* could regulate prostatic sensitivity to progressively increasing activation of angiogenesis signaling, we quantified VEGF production in response to vanadate, an inducer of the PI3K–HIF-1α–VEGF pathway in prostate cancer cells (34). Exposure of an $Ahr^{+/-}$ TRAMP dorsolateral prostate in organ culture to 100 μM vanadate resulted in a time-dependent increase in VEGF secretion

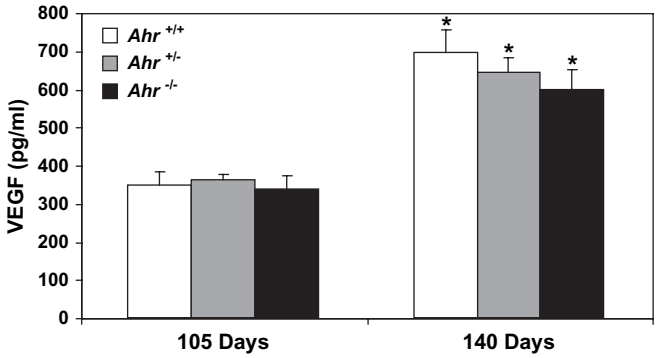

Fig. 1. VEGF concentrations in $Ahr^{+/+}$, $Ahr^{+/-}$ and $Ahr^{-/-}$ C57BL/6J TRAMP mouse dorsolateral prostates at 105 and 140 days of age. VEGF concentrations were determined by enzyme immunoassay on 40 μg total protein isolated from dorsolateral prostate tissue homogenates ($n = 6$ for each *Ahr* genotype at 105 and 140 days of age). *significantly different than VEGF concentrations in dorsolateral prostates of the same *Ahr* genotype at 105 days of age ($P < 0.05$).

into the culture media (Figure 2). VEGF secretion was also induced in a linear fashion over time in $Ahr^{+/+}$ and $Ahr^{-/-}$ TRAMPs (results not shown). These results show that vanadate also induced VEGF production in cultured TRAMPs.

VEGF concentrations in organ culture media of $Ahr^{+/+}$, $Ahr^{+/-}$ and $Ahr^{-/-}$ TRAMP mouse dorsolateral prostates exposed to vanadate

Having shown that VEGF production in the TRAMP can be stimulated by vanadate exposure, we next determined how induction was regulated by the *Ahr.* VEGF concentrations in culture media from TRAMP dorsolateral prostates exposed to vehicle alone did not differ based on *Ahr* genotype (Figure 3A). Thus, we surmised that *Ahr* genotype would not influence the degree of vanadate responsiveness. In cultured TRAMPs exposed to vanadate, VEGF concentrations were induced in a dose-dependent manner only in $Ahr^{+/-}$ and $Ahr^{-/-}$ TRAMP cultures (Figure 3B). However, the maximum level of VEGF induction exceeded the induction observed in $Ahr^{+/+}$ TRAMPs in only $Ahr^{-/-}$ TRAMP cultures. In dorsolateral prostate cultures from each *Ahr* genotype, vanadate-induced VEGF production was inhibited by wortmannin, an inhibitor of PI3K activation. Thus, these results demonstrate that unlike $Ahr^{+/-}$ and $Ahr^{-/-}$ TRAMPs, $Ahr^{+/+}$ TRAMPs are relatively resistant to vanadate induction of VEGF and confirming a previous report that this activation occurs through the PI3K-signaling cascade (34).

Vanadate activation of the PI3K-signaling cascade in $Ahr^{+/+}$, $Ahr^{+/-}$ and $Ahr^{-/-}$ TRAMP mouse dorsolateral prostates

Although vanadate-induced VEGF production occurred to a greater extent in $Ahr^{-/-}$ TRAMPs than those from $Ahr^{+/+}$ and $Ahr^{+/-}$ TRAMPs, it was still necessary to determine if vanadate induced PI3K signaling upstream of VEGF in TRAMPs of all *Ahr* genotypes. To quantify vanadate stimulation of the PI3K pathway upstream of HIF-1α, we measured protein phosphorylation of Akt by western blot. Total Akt protein levels did not differ significantly in $Ahr^{+/+}$, $Ahr^{+/-}$ and $Ahr^{-/-}$ TRAMP dorsolateral prostates exposed to vehicle in culture, nor did they differ in prostates from any *Ahr* genotype upon exposure to vanadate (Figure 4A). Thus, greater sensitivity to VEGF production in $Ahr^{-/-}$ TRAMP dorsolateral prostates exposed to vanadate could not be explained by inherently elevated Akt protein expression. However, activation of PI3K signaling, detected by phosphorylation of Akt, was elevated in all $Ahr^{+/+}$, $Ahr^{+/-}$ and $Ahr^{-/-}$ TRAMP dorsolateral prostates exposed to vanadate in culture compared with vehicle-exposed prostates (Figure 4B). Phosphorylated Akt band density was similar in dorsolateral prostates of each *Ahr* genotype in the presence of vehicle alone, and the magnitude of induction in prostates from each *Ahr* genotype was comparable after vanadate exposure. These results suggest that greater sensitivity to stimulation of VEGF production in $Ahr^{-/-}$ TRAMP dorsolateral prostates occurs at some point downstream of Akt activation.

HIF-1α and ARNT protein levels in cultured $Ahr^{+/+}$, $Ahr^{+/-}$ and $Ahr^{-/-}$ TRAMP mouse dorsolateral prostates exposed to vanadate

While activation of PI3K signaling through phosphorylation of Akt was similar in vanadate-exposed $Ahr^{+/+}$, $Ahr^{+/-}$ and $Ahr^{-/-}$ TRAMP dorsolateral prostates, it was still undetermined if greater VEGF activation in $Ahr^{-/-}$ TRAMPs could be attributed to greater protein levels of proteins further downstream. This could be explained by either elevated background protein levels of HIF-1α or ARNT or by a greater susceptibility to vanadate induction of these proteins in $Ahr^{-/-}$ TRAMP dorsolateral prostates. HIF-1α protein levels determined by enzyme-linked immunosorbent assay analysis were not significantly different in $Ahr^{+/+}$, $Ahr^{+/-}$ and $Ahr^{-/-}$ TRAMP dorsolateral prostates exposed to either vehicle or vanadate (Figure 5A). Western blot analysis demonstrated that ARNT protein levels did not differ as a function of *Ahr* genotype or vanadate exposure (Figure 5B).

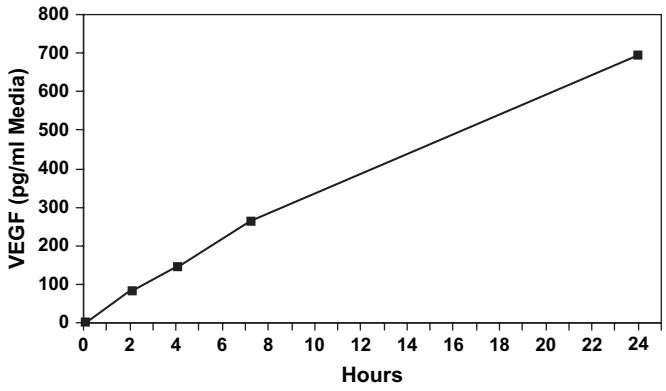

Fig. 2. Vanadate induction of VEGF in organ culture media over time. VEGF concentrations were determined in organ culture media of an $Ahr^{+/-}$ TRAMP dorsolateral prostate exposed to 100 μM vanadate for 24 h. VEGF concentrations were determined by enzyme immunoassay on aliquots of organ culture media taken at 2, 4, 7.25 and 24 h from the same culture.

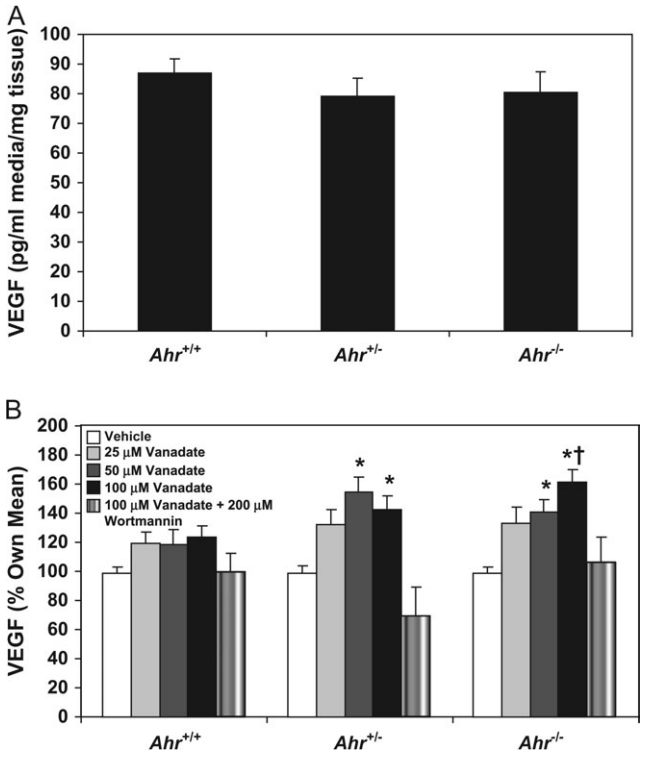

Fig. 3. Vanadate induction of VEGF in organ culture media of $Ahr^{+/+}$, $Ahr^{+/-}$ and $Ahr^{-/-}$ C57BL/6J TRAMP mouse dorsolateral prostates. Dorsolateral prostates from $Ahr^{+/+}$ ($n = 12$), $Ahr^{+/-}$ ($n = 8$) and $Ahr^{-/-}$ ($n = 11$) C57BL/6J TRAMP mice were cultured for 3 days, with media changed every 24 h. Approximately 2–4 mg from each dorsolateral prostate was cultured in duplicate in media containing 0, 25, 50 or 100 μM vanadate or 100 μM vanadate plus 200 μM wortmannin. VEGF concentrations were measured by enzyme immunoassay in organ culture media obtained from media collected from the final 24 h incubation period. The mean VEGF concentration for each dose of vanadate per mouse was used to calculate the mean VEGF concentration for $Ahr^{+/+}$, $Ahr^{+/-}$ and $Ahr^{-/-}$ C57BL/6J TRAMP mouse dorsolateral prostates. VEGF concentrations for $Ahr^{+/+}$, $Ahr^{+/-}$ and $Ahr^{-/-}$ C57BL/6J TRAMP mouse dorsolateral prostates cultured in the absence of vanadate (**A**), and the magnitude of induction in response to vanadate (**B**) is shown. *significantly different than VEGF concentrations in culture media from dorsolateral prostates of the same *Ahr* genotype ($P < 0.05$). †significantly different than VEGF concentrations in $Ahr^{+/+}$ C57BL/6J TRAMP mouse dorsolateral prostates exposed to 100 mM vanadate ($P < 0.05$)

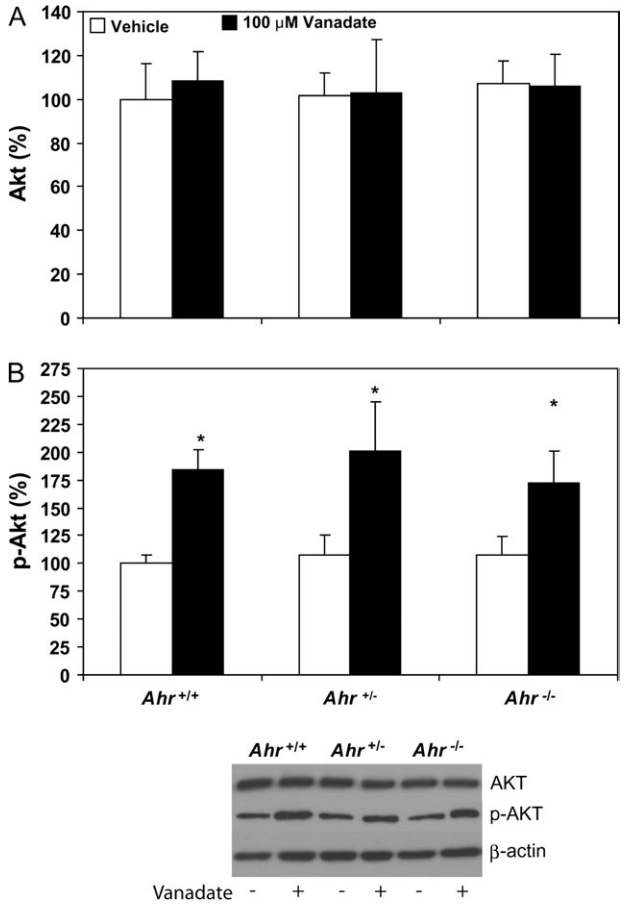

Fig. 4. Vanadate activation of the PI3K pathway in $Ahr^{+/+}$, $Ahr^{+/-}$ and $Ahr^{-/-}$ C57BL/6J TRAMP mouse dorsolateral prostates. Western blot determination of Akt (**A**) and p-Akt (**B**) protein band density was determined using 10 μg total protein isolated from dorsolateral prostate tissue homogenates cultured with vehicle or 100 μM vanadate ($n = 6$ for each group and each *Ahr* genotype). Band density was calculated for each protein and expressed relative to band density of b-actin. *significantly different than p-AKT levels in dorsolateral prostates of the same Ahr genotype ($P < 0.05$).

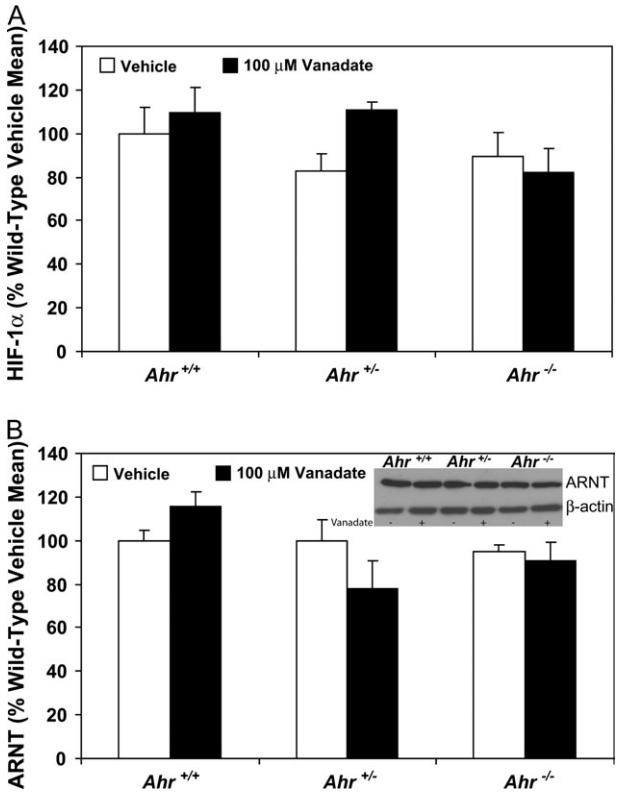

Fig. 5. HIF-1a and ARNT protein levels in $Ahr^{+/+}$, $Ahr^{+/-}$ and $Ahr^{-/-}$ C57BL/6J TRAMP mouse dorsolateral prostate organ cultures. HIF-1a protein levels (**A**) were determined by enzyme immunoassay on 10 μg total protein isolated from tissue homogenates obtained from dorsolateral prostates cultured with vehicle or 100 μM vanadate ($n = 5$ for $Ahr^{+/+}$ and $n = 3$ for $Ahr^{+/-}$ and $Ahr^{-/-}$ prostates). ARNT protein levels (**B**) were determined by western blot analysis of 10 μg total protein isolated from dorsolateral prostate tissue homogenates cultured with vehicle or 100 μM vanadate ($n = 3$ for each group and each Ahr genotype). Band density was calculated for each protein and expressed relative to b-actin band density.

Discussion

The TRAMP model has proven to be an invaluable resource for investigating the role of the AhR in prostate carcinogenesis. We have shown previously that presence of the *Ahr* inhibits prostate tumor formation, as TRAMP mice lacking the *Ahr* ($Ahr^{-/-}$) developed neuroendocrine prostate tumors with greater frequency than $Ahr^{+/+}$ TRAMP mice (30). We observed that all mice developed diffuse epithelial prostate hyperplasia commonly associated with the TRAMP model by 105 days, but macroscopic tumor formation was inhibited by the AhR (30). However, it is difficult to conclusively determine the molecular changes occurring prior to tumor formation that are responsible for tumor growth simply by comparing molecular markers in prostate tumors and tumor-free prostates. In the current study, we utilize a tissue culture model that maintains the natural tissue microenvironment of these hyperplastic prostates to determine how production of factors responsible for tumor growth is regulated by the AhR. We show that the production of VEGF, a key regulator of tissue angiogenesis and tumor growth, is inhibited in TRAMPs by the AhR prior to tumor formation.

Here, we demonstrate a significant increase in prostate VEGF concentrations between 105 and 140 days of age, when tumor incidence is increasing, albeit to a greater extent in $Ahr^{-/-}$ TRAMP mice. This observation is consistent with a previous report that VEGF messenger RNA expression is elevated in hyperplastic TRAMPs, and VEGF protein levels are elevated during progressive tumor growth (32). VEGF expression has also been associated with disease progression in men with prostate cancer (9,31). However, it was unclear why VEGF concentrations increased equally in all TRAMPs, particularly in $Ahr^{-/-}$ TRAMP mice that subsequently develop more prostate tumors than $Ahr^{+/-}$ and $Ahr^{-/-}$ TRAMP mice.

To determine the underlying mechanisms responsible for the greater proclivity of $Ahr^{-/-}$ prostates to develop prostate tumors, it was first necessary to characterize responsiveness to signals that would account for elevated VEGF. One of the major signaling pathways responsible for VEGF production is mediated by HIF-1α. This pathway is associated with facilitating growth of preneoplastic lesions by establishing vascular networks required for tumor growth. Hypoxic conditions during accelerated epithelial growth in preneoplastic regions stabilize or upregulate HIF-1α, facilitating local production of angiogenic factors (32). Using vanadate to stimulate this pathway (34), we observed a significant increase in VEGF production in $Ahr^{-/-}$ TRAMPs and found that $Ahr^{+/+}$ TRAMPs were resistant to this induction. However, both $Ahr^{-/-}$ and $Ahr^{+/+}$ TRAMPs showed increased phosphorylation of Akt following vanadate exposure, indicative of induction of PI3K signaling. Furthermore, protein levels of HIF-1α and ARNT were similar in $Ahr^{+/+}$, $Ahr^{+/-}$ and $Ahr^{-/-}$ TRAMPs, so altered sensitivity to VEGF production could not be solely attributed to greater levels of downstream proteins in the cascade. These findings are consistent with PI3K activation of VEGF, although it was also shown that HIF-1α protein levels were also induced in prostate cancer cells (34). However, it is probable that hyperplastic prostates in culture already have stabilized HIF-1α so that

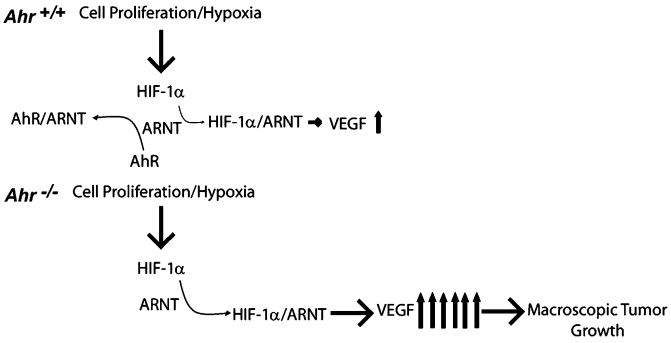

Fig. 6. Proposed mechanism responsible for VEGF regulation by the AhR in the TRAMP. When the AhR is present in TRAMP mice with diffuse epithelial hyperplasia, the AhR would interact with and sequester ARNT, minimizing the ability of ARNT to interact with stabilized HIF-1 to induce VEGF production. The net effect would be to effectively diminish likelihood of tumor growth. When the AhR is absent, ARNT would be free to interact with stabilized HIF-1 to stimulate VEGF production, resulting in a greater likelihood of tumor growth.

greater induction in response to vanadate does not occur as it does in cells. These findings indicate that the presence of the AhR impairs the sensitivity of the TRAMP to signals that are responsible for VEGF production.

Although we have shown that the AhR diminishes VEGF production in the TRAMP exposed to vanadate, the biological significance in prostate carcinogenesis is unclear. VEGF induction through activation of the PI3K pathway can also be caused by other upstream signals, including reactive oxygen species, growth factors and cytokines that are implicated in prostate carcinogenesis (15,16,34,37). Furthermore, circumvention of repressed PI3K signaling by loss of phosphatase and tensin homolog is commonly found in prostate carcinogenesis (38–44). Thus, regulation of VEGF production by the AhR through interaction with ARNT may inhibit multiple signaling cascades involved in prostate carcinogenesis. Likewise, the presence of the AhR and ARNT in many organs (45,46) does not exclude the possibility that HIF-1α activation that occurs in numerous other human cancers dependent on angiogenesis (17,18) could also be inhibited by AhR interaction with ARNT.

Based on our observations, we propose that the AhR regulates VEGF production through sequestering ARNT, thereby limiting interaction with stabilized HIF-1α (Figure 6). In the presence of the diffuse epithelial hyperplasia found in all TRAMPs, AhR interacts with ARNT to inhibit the ability of stabilized HIF-1α to induce VEGF production, resulting in less tumor growth. When the AhR is absent, unimpeded HIF-1α–ARNT interaction stimulates VEGF production leading to greater prevalence for tumor formation. The AhR–ARNT interaction would probably minimize VEGF production and tumor growth caused by a hypoxic environment caused by excessive prostate cell proliferation or by increased production of growth factors previously implicated in prostate carcinogenesis (15,16,34,37). This effect would not minimize activation of the PI3K-signaling pathway *per se*, but would reduce the physiologic response of VEGF production and subsequent tumor growth downstream of HIF-1α activation.

Regulation of VEGF production by the AhR has been described previously, as AhR-null mice develop cardiac hypertrophy as a result of greater HIF-1α levels and a subsequent increase in VEGF messenger RNA abundance (33). It has also been shown that ligand activation of the AhR inhibits neovascularization in mice (47,48). Similarly, inhibition of coronary vasculogenesis in chick embryos can be rescued by VEGF exposure (49). In the current study, it is uncertain what mechanisms are responsible for facilitating AhR interaction with ARNT, namely AhR nuclear localization in the absence of dioxins. It is possible that nuclear localization results from interaction with an endogenous ligand (20,21) or through some additional mechanism that remains to be determined. Regardless, it appears that both the AhR in the absence of ligand and ligand-activated AhR can have profound effects on vasculature development. This raises the intriguing possibility that low-affinity AhR ligands that lack toxicity of more potent AhR ligands could have therapeutic potential against prostate carcinogenesis.

Selective AhR modulators, lacking the AhR-mediated toxicity associated with dioxin exposure (50), have been shown to inhibit prostate cancer cell growth (51,52). These results suggest that stimulation of the AhR pathway could enhance the sequestering effects of the AhR through interaction with ARNT and inhibit prostate carcinogenesis *in vivo*. Potential prostate tumor inhibition by selective AhR modulators is currently being explored.

Funding

National Cancer Institute (CA095751); National Institutes of Health (ES01332, ES12352).

Acknowledgements

The authors would like to thank Dr Michelle Cotroneo for her assistance with preparation of this manuscript.

Conflict of Interest Statement: None declared.

References

1. Jemal,A. *et al*. (2007) Cancer statistics, 2007. *CA Cancer J. Clin.*, **57**, 43–66.
2. Abate-Shen,C. *et al*. (2000) Molecular genetics of prostate cancer. *Genes Dev.*, **14**, 2410–2434.
3. DeMarzo,A.M. *et al*. (2003) Pathological and molecular aspects of prostate cancer. *Lancet*, **361**, 955–964.
4. Feldman,B.J. *et al*. (2001) The development of androgen-independent prostate cancer. *Nat. Rev. Cancer*, **1**, 34–45.
5. Grossmann,M.E. *et al*. (2001) Androgen receptor signaling in androgen-refractory prostate cancer. *J. Natl Cancer Inst.*, **93**, 1687–1697.
6. Cox,M.C. *et al*. (2005) Angiogenesis and prostate cancer: important laboratory and clinical findings. *Curr. Oncol. Rep.*, **7**, 215–219.
7. Lara,P.N.Jr *et al*. (2004) Angiogenesis-targeted therapies in prostate cancer. *Clin. Prostate Cancer*, **3**, 165–173.
8. Ferrara,N. *et al*. (1997) The biology of vascular endothelial growth factor. *Endocr. Rev.*, **18**, 4–25.
9. Harper,M.E. *et al*. (1996) Vascular endothelial growth factor (VEGF) expression in prostatic tumours and its relationship to neuroendocrine cells. *Br. J. Cancer*, **74**, 910–916.
10. Borre,M. *et al*. (2000) Association between immunohistochemical expression of vascular endothelial growth factor (VEGF), VEGF-expressing neuroendocrine-differentiated tumor cells, and outcome in prostate cancer patients subjected to watchful waiting. *Clin. Cancer Res.*, **6**, 1882–1890.
11. Ferrer,F.A. *et al*. (1997) Vascular endothelial growth factor (VEGF) expression in human prostate cancer: *in situ* and *in vitro* expression of VEGF by human prostate cancer cells. *J. Urol.*, **157**, 2329–2333.
12. Jones,A. *et al*. (2000) Elevated serum vascular endothelial growth factor in patients with hormone-escaped prostate cancer. *BJU Int.*, **85**, 276–280.
13. Forsythe,J.A. *et al*. (1996) Activation of vascular endothelial growth factor gene transcription by hypoxia-inducible factor 1. *Mol. Cell. Biol.*, **16**, 4604–4613.
14. Marti,H.H. *et al*. (1998) Systemic hypoxia changes the organ-specific distribution of vascular endothelial growth factor and its receptors. *Proc. Natl Acad. Sci. USA*, **95**, 15809–15814.
15. Jiang,B.H. *et al*. (2001) Phosphatidylinositol 3-kinase signaling controls levels of hypoxia-inducible factor 1. *Cell Growth Differ.*, **12**, 363–369.
16. Zhong,H. *et al*. (2000) Modulation of hypoxia-inducible factor 1alpha expression by the epidermal growth factor/phosphatidylinositol 3-kinase/PTEN/AKT/FRAP pathway in human prostate cancer cells: implications for tumor angiogenesis and therapeutics. *Cancer Res.*, **60**, 1541–1545.
17. Semenza,G.L. (2003) Targeting HIF-1 for cancer therapy. *Nat. Rev. Cancer*, **3**, 721–732.
18. Fresno Vara,J.A. *et al*. (2004) PI3K/Akt signalling pathway and cancer. *Cancer Treat. Rev.*, **30**, 193–204.
19. Hankinson,O. (1995) The aryl hydrocarbon receptor complex. *Annu. Rev. Pharmacol. Toxicol.*, **35**, 307–340.

20. Song,J. *et al*. (2002) A ligand for the aryl hydrocarbon receptor isolated from lung. *Proc. Natl Acad. Sci. USA*, **99**, 14694–14699.
21. Henry,E.C. *et al*. (2006) A potential endogenous ligand for the aryl hydrocarbon receptor has potent agonist activity *in vitro* and *in vivo*. *Arch. Biochem. Biophys.*, **450**, 67–77.
22. Kashani,M. *et al*. (1998) Expression of the aryl hydrocarbon receptor (AhR) and the aryl hydrocarbon receptor nuclear translocator (ARNT) in fetal, benign hyperplastic, and malignant prostate. *Prostate*, **37**, 98–108.
23. Fernandez-Salguero,P. *et al*. (1995) Immune system impairment and hepatic fibrosis in mice lacking the dioxin-binding Ah receptor. *Science*, **268**, 722–726.
24. Schmidt,J.V. *et al*. (1996) Characterization of a murine Ahr null allele: involvement of the Ah receptor in hepatic growth and development. *Proc. Natl Acad. Sci. USA*, **93**, 6731–6736.
25. Mimura,J. *et al*. (1997) Loss of teratogenic response to 2,3,7,8-tetrachlorodibenzo-*p*-dioxin (TCDD) in mice lacking the Ah (dioxin) receptor. *Genes Cells*, **2**, 645–654.
26. Greenberg,N.M. *et al*. (1995) Prostate cancer in a transgenic mouse. *Proc. Natl Acad. Sci. USA*, **92**, 3439–3443.
27. Gingrich,J.R. *et al*. (1996) Metastatic prostate cancer in a transgenic mouse. *Cancer Res.*, **56**, 4096–4102.
28. Gingrich,J.R. *et al*. (1997) Androgen-independent prostate cancer progression in the TRAMP model. *Cancer Res.*, **57**, 4687–4691.
29. Hsu,C.X. *et al*. (1998) Longitudinal cohort analysis of lethal prostate cancer progression in transgenic mice. *J. Urol.*, **160**, 1500–1505.
30. Fritz,W.A. *et al*. (2007) The aryl hydrocarbon receptor inhibits prostate carcinogenesis in TRAMP mice. *Carcinogenesis*, **28**, 497–505.
31. Kaplan-Lefko,P.J. *et al*. (2003) Pathobiology of autochthonous prostate cancer in a pre-clinical transgenic mouse model. *Prostate*, **55**, 219–237.
32. Huss,W.J. *et al*. (2001) Angiogenesis and prostate cancer: identification of a molecular progression switch. *Cancer Res.*, **61**, 2736–2743.
33. Thackaberry,E.A. *et al*. (2002) Aryl hydrocarbon receptor null mice develop cardiac hypertrophy and increased hypoxia-inducible factor-1alpha in the absence of cardiac hypoxia. *Cardiovasc. Toxicol.*, **2**, 263–274.
34. Gao,N. *et al*. (2002) Vanadate-induced expression of hypoxia-inducible factor 1 alpha and vascular endothelial growth factor through phosphatidylinositol 3-kinase/Akt pathway and reactive oxygen species. *J. Biol. Chem.*, **277**, 31963–31971.
35. Benedict,J.C. *et al*. (2000) Physiological role of the aryl hydrocarbon receptor in mouse ovary development. *Toxicol. Sci.*, **56**, 382–388.
36. Lin,T.-M. *et al*. (2002) Effects of aryl hydrocarbon receptor null mutation and *in utero* and lactational 2,3,7,8-tetrachlorodibenzo-*p*-dioxin exposure on prostate and seminal vesicle development in C57BL/6 mice. *Toxicol. Sci.*, **68**, 479–487.
37. Hsing,A.W. *et al*. (2001) Prostate cancer risk and serum levels of insulin and leptin: a population-based study. *J. Natl Cancer Inst.*, **93**, 783–789.
38. Ali,I.U. *et al*. (1999) Mutational spectra of PTEN/MMAC1 gene: a tumor suppressor with lipid phosphatase activity. *J. Natl Cancer Inst.*, **91**, 1922–1932.
39. Li,J. *et al*. (1997) PTEN, a putative protein tyrosine phosphatase gene mutated in human brain, breast, and prostate cancer. *Science*, **275**, 1943–1947.
40. Steck,P.A. *et al*. (1997) Identification of a candidate tumour suppressor gene, MMAC1, at chromosome 10q23.3 that is mutated in multiple advanced cancers. *Nat. Genet.*, **15**, 356–362.
41. Teng,D.H. *et al*. (1997) MMAC1/PTEN mutations in primary tumor specimens and tumor cell lines. *Cancer Res.*, **57**, 5221–5225.
42. Cantley,L.C. *et al*. (1999) New insights into tumor suppression: PTEN suppresses tumor formation by restraining the phosphoinositide 3-kinase/AKT pathway. *Proc. Natl Acad. Sci. USA*, **96**, 4240–4245.
43. Di Cristofano,A. *et al*. (2000) The multiple roles of PTEN in tumor suppression. *Cell*, **100**, 387–390.
44. Kwabi-Addo,B. *et al*. (2001) Haploinsufficiency of the Pten tumor suppressor gene promotes prostate cancer progression. *Proc. Natl Acad. Sci. USA*, **98**, 11563–11568.
45. Carver,L.A. *et al*. (1994) Tissue specific expression of the rat Ah-receptor and ARNT mRNAs. *Nucleic Acids Res.*, **22**, 3038–3044.
46. Roman,B.L. *et al*. (1998) Responsiveness of the adult male rat reproductive tract to 2,3,7,8-tetrachlorodibenzo-*p*-dioxin exposure: Ah receptor and ARNT expression, CYP1A1 induction, and Ah receptor down-regulation. *Toxicol. Appl. Pharmacol.*, **150**, 228–239.
47. Lin,T.M. *et al*. (2001) Role of the aryl hydrocarbon receptor in the development of control and 2,3,7,8-tetrachlorodibenzo-*p*-dioxin-exposed male mice. *J. Toxicol. Environ. Health A*, **64**, 327–342.
48. Thackaberry,E.A. *et al*. (2005) Effect of 2,3,7,8-tetrachlorodibenzo-*p*-dioxin on murine heart development: alteration in fetal and postnatal cardiac growth, and postnatal cardiac chronotropy. *Toxicol. Sci.*, **88**, 242–249.
49. Ivnitski-Steele,I.D. *et al*. (2003) Vascular endothelial growth factor rescues 2,3,7,8-tetrachlorodibenzo-p-dioxin inhibition of coronary vasculogenesis. *Birth Defects Res. A Clin. Mol. Teratol.*, **67**, 496–503.
50. Piskorska-Pliszczynska,J. *et al*. (1991) Mechanism of action of 2,3,7,8-tetrachlorodibenzo-*p*-dioxin antagonists: characterization of 6-[125I]-methyl-8-iodo-1,3-dichlorodibenzofuran-Ah receptor complexes. *Arch. Biochem. Biophys.*, **284**, 193–200.
51. Morrow,D. *et al*. (2004) Aryl hydrocarbon receptor-mediated inhibition of LNCaP prostate cancer cell growth and hormone-induced transactivation. *J. Steroid Biochem. Mol. Biol.*, **88**, 27–36.
52. Nachshon-Kedmi,M. *et al*. (2004) Induction of apoptosis in human prostate cancer cell line, PC3, by 3,3′-diindolylmethane through the mitochondrial pathway. *Br. J. Cancer*, **91**, 1358–1363.

Received June 26, 2007; revised March 4, 2008; accepted March 8, 2008